Progress In Electromagnetics Research C, Vol. 77, 29–38, 2017

A Compact MIMO/Diversity Antenna with WLAN Band-Notch Characteristics for Portable UWB Applications

Shrivishal Tripathi[1, *], Akhilesh Mohan[2], and Sandeep Yadav[3]

Abstract—In this paper, a compact multiple-input-multiple-output (MIMO)/diversity antenna with WLAN band notch characteristics, high isolation, and good ECC suitable for portable ultra-wideband (UWB) applications is presented. The proposed antenna has optimized dimensions of 29 mm × 38 mm. The antenna consists of two orthogonal circular monopoles with a 50 Ω microstrip feed line. In addition, to enhance the impedance bandwidth, a fractal slot, created using Minkowski fractal geometry, is introduced into the ground plane, which is located on the other side of the substrate, just below the feed line. Good isolation ($\geq$ 21.5 dB) with a fractional bandwidth up to 220% is achieved between antenna elements by introducing two ground stubs and a rectangular slot in the ground plane. A band-notch characteristic in the WLAN band is obtained by etching an elliptical split-ring resonator (ESRR) in the radiator. Moreover, a diversity performance of the antenna in terms of ECC (< 0.01) and capacity loss (< 0.3 b/s/Hz) is performed. This paper offers, for the first time, a combined effect of fractal geometry and ESRR geometry in an antenna design. Finally, a comparison of the proposed antenna is performed with the UWB MIMO/diversity antennas existing in the literature. These results show the suitability of the presented antenna for portable UWB systems.

1. INTRODUCTION

The ultra-wideband (UWB) technology has been rapidly growing following the authorization of the unlicensed use from the Federal Communication Commission (FCC) in 2002, and it operates in 3.1–10.6 GHz frequency spectrum [1]. It has gained the attention of researchers due to a number of key features such as high data transmission capacity, very low power, and compact dimensions. A UWB system, however, is susceptible to multipath fading problems as other systems. Thus, multiple-input-multiple-output (MIMO) technology can be used to improve diversity gain and multipath fading [2, 3]. UWB MIMO/diversity technology requires high isolation among antenna elements to combat multipath fading problem. However, a compact UWB MIMO/diversity antenna for portable applications in a smaller area causes degradation in diversity performance due to the presence of various mutual coupling effects among the antenna elements. Existing narrowband systems such as wireless local area network (WLAN), in 5.15–5.825 GHz, operate in the UWB spectrum and cause severe interference issues in the UWB spectrum. Thus, the design of a compact UWB MIMO/diversity antenna which has band rejection characteristics is a very challenging task.

A UWB antenna with MIMO/diversity technology has been proposed in the literature to resolve issues such as wideband isolation, compact size, and filtering of interference band [4–10]. In [4, 5], decoupling structures are placed between monopoles to enhance the isolation. The band-notch

Received 20 April 2017, Accepted 8 August 2017, Scheduled 17 August 2017

* Corresponding author: Shrivishal Tripathi (shrivishal@iitj.ac.in).

[1] Department of Electronics and Communication Engineering, International Institute of Information Technology Naya Raipur, Chhatisgarh 221005, India. [2] Department of Electronics and Electrical Communication, Indian Institute of Technology Kharagpur, West Bengal 721302, India. [3] Department of Electrical Engineering, Indian Institute of Technology Jodhpur, Rajasthan 342011, India.

characteristic in the UWB is achieved by etching different geometrical structures either from the monopole or the ground plane of the proposed wideband antenna structure. In [6], split-ring resonators geometry is used in the proposed antenna design, which helps to get the desired band rejection, whereas in [7] and [8], open loop resonators and U-shaped geometries are used, respectively, to obtain band rejection. However, the application of such structures in the design causes an increment in mutual coupling in the design, which affects band rejection behavior of the antenna. UWB MIMO/diversity antennas with band rejection in WLAN band are studied in [9, 10]. In the study presented in [11, 12], compact UWB MIMO/diversity antennas are reported, but these antennas, with an acceptable isolation and operational bandwidth, did not offer the band-notch characteristic. Therefore, designing a compact UWB MIMO/diversity antenna with good isolation, bandwidth, and band-notch characteristics is very difficult.

In this paper, a compact UWB MIMO/diversity antenna, with WLAN band notch characteristics, high isolation, and good ECC, is proposed, and its characteristics are investigated. It has a compact size of 29 mm × 38 mm. In this antenna, two circular monopoles (CMs) are placed orthogonal to each other. It helps to achieve a good isolation between the antennas monopoles, when the multiple monopoles are placed in close surroundings of each other. Through two ground stubs and a rectangular slot, isolation better than 21.5 dB is obtained in the entire UWB. Moreover, the band-notch characteristics in the desired WLAN band are obtained by etching an elliptical split-ring resonator (ESRR) shaped slot from each CM. This paper offers a combined effect of fractal geometry and ESRR geometry in antenna geometry. The simulated and measured results show that the proposed UWB MIMO/diversity antenna is an appropriate candidate for portable UWB systems.

2. ANTENNA DESIGN

2.1. Antenna Configuration

The proposed optimized geometry of the UWB MIMO/diversity antenna, the design and analysis of which is carried out using Ansoft HFSS v.13, is presented in Figure 1. It has compact dimensions of 29 mm × 38 mm × 1.6 mm. The optimized antenna is fabricated on an FR4 substrate with a dielectric constant of 4.4 and loss tangent of 0.02. CM1 and CM2 monopoles of the MIMO/diversity antenna with their respective 50 Ω microstrip feed lines are printed on one side of the substrate, whereas the

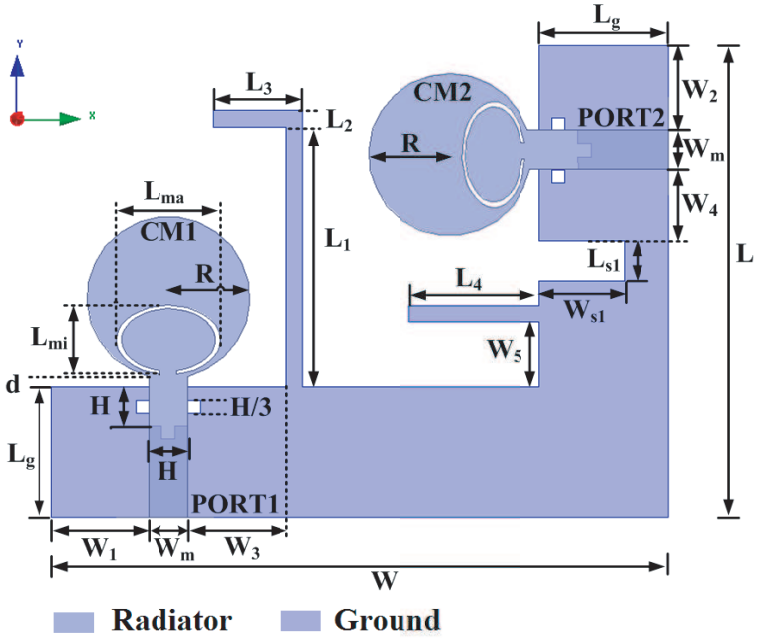

Figure 1. The geometry of the proposed UWB MIMO/diversity antenna.

ground plane is printed on the other side. CM1 and CM2 are oriented perpendicular to each other to obtain a good isolation between them [13]. The two monopoles are identical with radius R. A wideband isolation better than 21.5 dB is achieved with two stubs, which are extended from the ground plane.

It has been demonstrated in the literature that by etching a rectangular slot [14, 15] and an L-shaped slot [16] in the ground plane, a bandwidth up to 125% can be achieved. Therefore, a fractal slot and a rectangular slot are inserted in the ground plane of the antenna. The band-notch characteristics in the desired WLAN band are achieved by introducing an ESRR shaped slot in each of the CMs. The optimized dimensions of the antenna are: $L = 29\,\text{mm}$, $W = 38\,\text{mm}$, $R = 5\,\text{mm}$, $W_m = 2.4\,\text{mm}$, $L_g = 8\,\text{mm}$, $d = 0.6\,\text{mm}$, $H = 2.4\,\text{mm}$, $w = 0.3\,\text{mm}$, $L_1 = 16\,\text{mm}$, $L_2 = 1\,\text{mm}$, $L_3 = 5.5\,\text{mm}$, $L_4 = 8\,\text{mm}$, $W_1 = 6\,\text{mm}$, $W_2 = 5\,\text{mm}$, $W_3 = 6.1\,\text{mm}$, $W_4 = 4.5\,\text{mm}$, $W_5 = 4.5\,\text{mm}$, $L_{s1} = 2.5\,\text{mm}$, $W_{s1} = 5.25\,\text{mm}$, $L_{ma} = 6.4\,\text{mm}$, and $L_{mi} = 4\,\text{mm}$.

Figure 2. The iterative generation of the Minkowski fractal slot, (a) Iteration-0, (b) Iteration-1 and (c) Iteration-2.

2.2. Effect of Fractal Slot and Rectangular Slot

A fractal slot created using Minkowski fractal geometry is introduced in the ground plane, below the feed line. The introduction of the fractal slot helps to achieve the wideband performance as well as stable radiation patterns at higher frequencies [17]. The iteration wise generation of the fractal slot is presented in Figure 2. The effect of the fractal slot on S_{11}/S_{22} is displayed in Figure 3(a). It can be seen that the operating bandwidth enhancement at higher and lower edges of the operating band is due to multiple resonance phenomena of the fractals. Along with fractal slots, near to the ground plane of CM 2, a rectangular slot is also introduced in the antenna design. Here, the introduction of rectangular slots in the ground plane helps to improve the mutual coupling at lower and middle operating range of UWB spectrum, which is shown in Figure 3(b). It is seen that S_{21} (better than $-21.5\,\text{dB}$) performance of the antenna improves significantly in the UWB range.

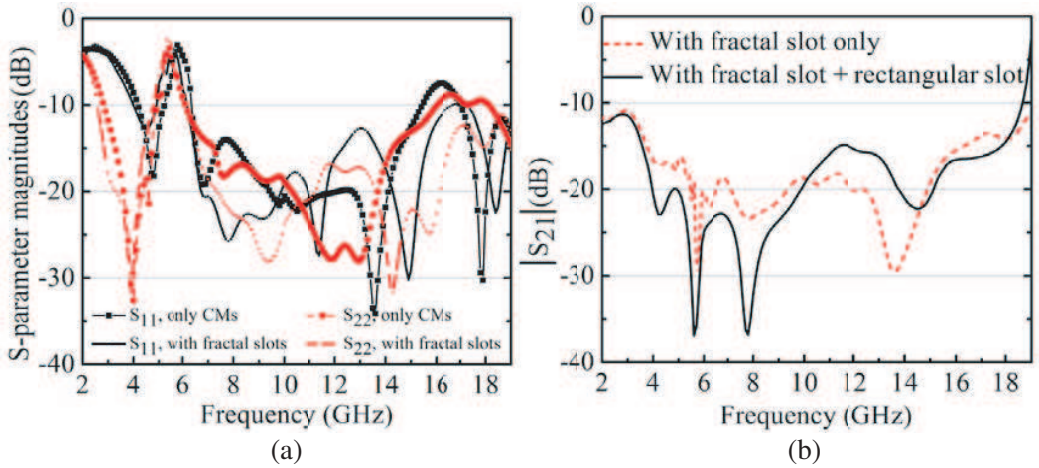

Figure 3. Simulated S_{11}, S_{22} and S_{12}/S_{21} characteristics of the fractal UWB MIMO/diversity antenna, (a) S_{11} and S_{22} with and without fractal slot, (b) S_{12}/S_{21} with and without rectangular slot.

2.3. Effect of Ground Stubs

In order to achieve improvement in isolation, L-shaped and I-shaped stubs are protruded from the ground plane of the UWB MIMO/diversity antenna by acting as wavetraps and. They work as a reflector which helps in improvement of the isolation by separating the radiation patterns of the CMs. The effects of these stubs on S-parameters are shown in Figure 4. It is observed from Figure 4(a) that after the introduction of stubs S_{11} and S_{22} performance at lower as well as at higher frequencies improves significantly. In Figure 4(b), with the grounded stub, one can see the improvement in isolation at lower as well as at higher operating frequencies, which helps to achieve the better isolation (> 21.5 dB) between CMs in the entire UWB. Moreover, the operating bandwidth is from 2.5–19 GHz with three resonant frequencies 4.1 GHz, 6.9 GHz and 9.4 GHz in the UWB.

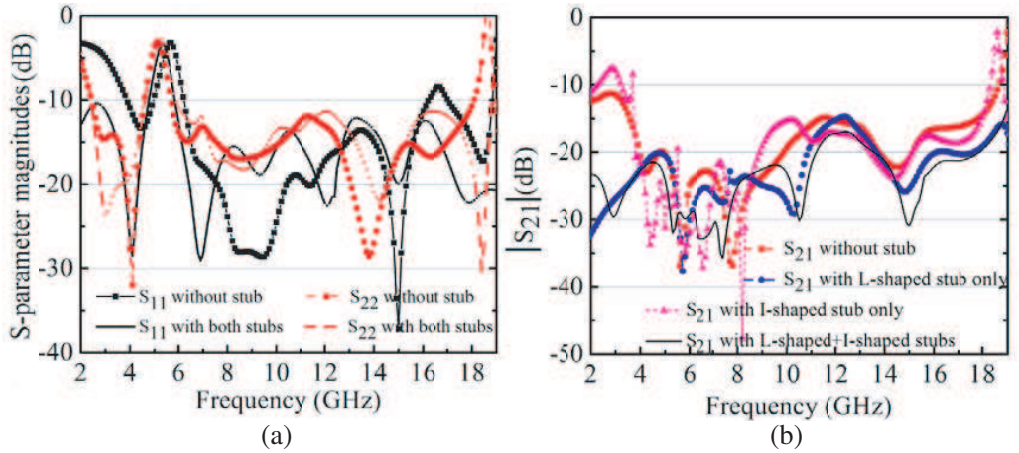

Figure 4. Simulated S_{11}, S_{22} and S_{12}/S_{21} characteristics of the MIMO/diversity antenna, (a) S_{11} and S_{22} with and without ground stub and (b) S_{12}/S_{21} with and without ground stub.

To further investigate the effect of stubs, surface current distributions of the UWB MIMO/diversity Antenna (UMA) at 9.4 GHz resonant frequency are shown in Figure 5. It can be seen that the flow of surface current from port 1 to port 2 has been reduced due to strong coupling of surface current with the grounded stubs. Stubs shapes and positions in the design is optimized in a way that it separate the radiations of the monopoles and affect the isolation maximally. This helps to enhance the isolation between the CMs.

2.4. Effect of Elliptical Split-Ring Resonator (ESRR)

In this study, an ESRR slot is etched from each CM to achieve the band-notch characteristics at WLAN band (5.15–5.85 GHz), centered at 5.5 GHz. These ESRR shaped slots are similar to monopoles and are used to provide the narrower and stronger notch-bands [18]. Moreover, the use of ESRR provides miniaturization of band notch structures, because an ellipse possesses a greater area than that of a corresponding circle, when the radius of the circle is equal to the semi-minor axis length of the ellipse. The notch length (L_n) of an ESRR slot of major axis length (L_{ma}), minor axis length (L_{mi}) and width (w) is calculated using following mathematical formula:

$$L_n = K\pi(0.5L_{mi} - w) \approx \frac{\lambda_g}{2} \approx \frac{c}{2f_{notch}\sqrt{\varepsilon_{eff}}} \tag{1}$$

$$K = 3(1+k) - \sqrt{(3+k)(1+3k)} \tag{2}$$

$$k = \frac{L_{ma}}{L_{mi}} \tag{3}$$

where, c represents the speed of light, λ_g the guided wavelength, ε_{eff} the effective dielectric constant as calculated in [19], K the ellipse circumference parameter, and k the axial ratio of the ellipse [20]. The

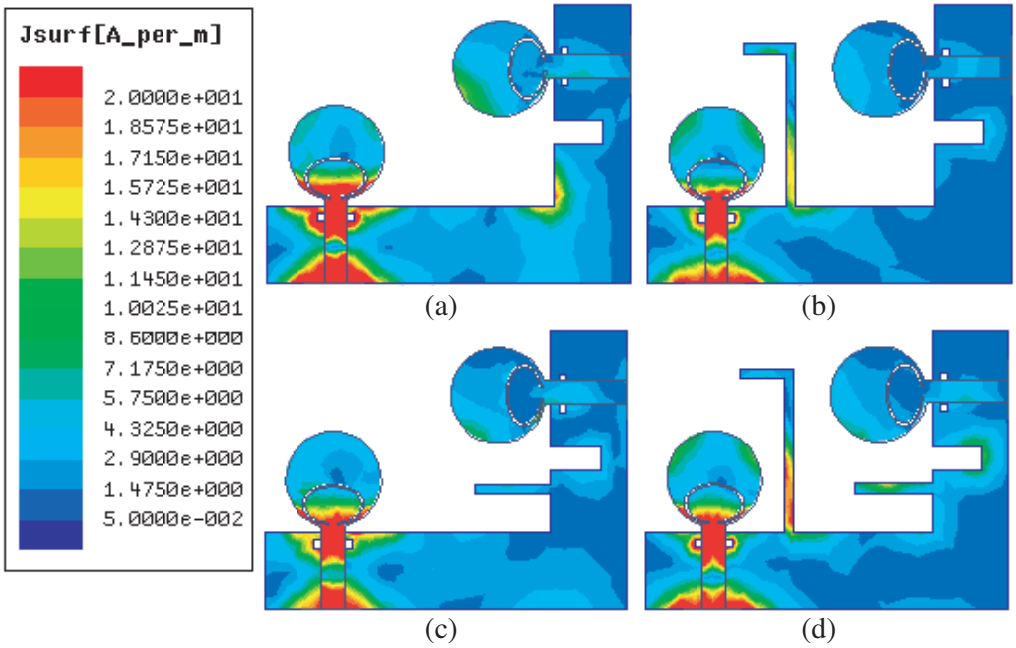

Figure 5. Surface current distribution (simulated) with port 1 excited at 9.4 GHz (a) without any stubs, (b) with L-shaped stub, (c) with I-shaped stub and (d) with L-shaped and I-shaped stubs.

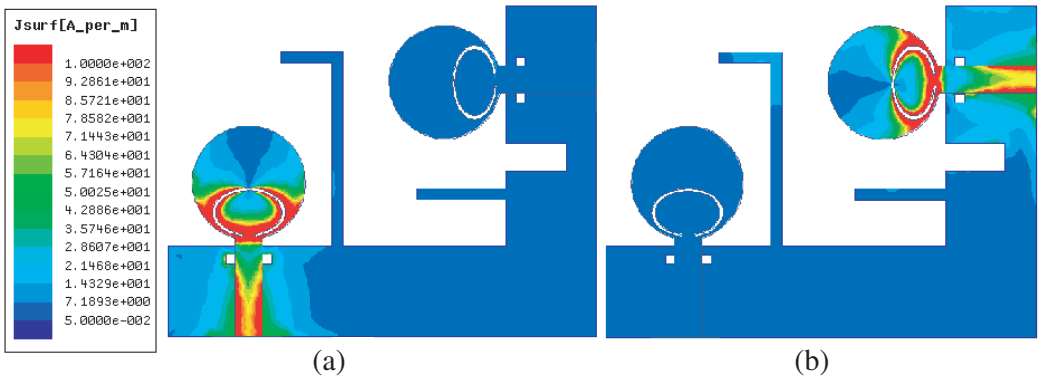

Figure 6. Surface current distribution (simulated) of proposed antenna at 5.5 GHz band notch frequency (a) when port 1 is excited, and (b) when port 2 is excited.

evaluated length of ESRR slot L_n using Eq. (1) is found to be 13.01 mm, whereas the actual length in the design is 14.06 mm. Here, actual length is close to calculated length. Figure 6 shows the simulated surface current distributions of the UMA at 5.5 GHz. It can be noticed that the intensity of surface current at the inner and the outer edges of ESRR is very strong, when port 1/port 2 is excited. This causes the suppression of radiation characteristics of the UMA at 5.5 GHz notch band.

3. RESULTS AND DISCUSSION

3.1. Impedance Performance

The designed UMA is fabricated in order to validate the feasibility of the prototype, and measurements are performed using the Agilent N9916A 14 GHz Field Fox Microwave Analyzer. Figure 7 displays the measured and simulated S-parameters. It can be seen from Figure 7(a) that measured S_{11} and S_{22}

responses are 2.6–14 GHz, excluding WLAN band in both the cases. It is seen from Figure 7(b) that an isolation of more than 21.5 dB is achieved for the entire UWB. Some differences between simulated and measured results are noticed due to soldering, use of SMA connectors and fabrication tolerances. In general, measured results are in good agreement with simulated results,though, some mismatch is observed due to asymmetrical placement of monopoles in the design as well as fabrication tolerances. In addition, the separation between the L-shaped stub and CM1 is less than the separation between the I-shaped and CM2. This asymmetrical placement of the geometries in the design will introduce capacitive loading with the grounded stub in the design, which in turn leads to lower cut off frequencies.

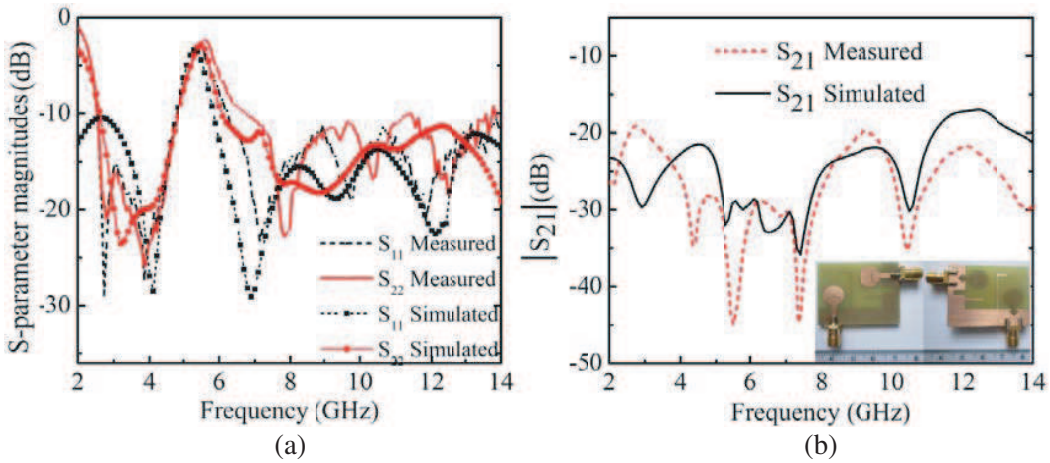

Figure 7. Comparison of measured and simulated S-parameters (a) S_{11} and S_{22}, and (b) S_{21}/S_{12}.

3.2. Radiation Performance

The radiation pattern of the UMA at 4.1, 6.9 and 9.4 GHz resonant frequencies in the E-plane (xz-plane) as well as in the H-plane (yz-plane) are shown in Figure 8. It can be seen that E-plane radiation pattern is almost symmetrical in nature. Moreover, radiation pattern behaviors in case of H-plane at lower resonant frequencies are almost similar to each other. During the measurement, when port 1 is excited, then port 2 is matched by a 50 Ω load, and vice versa. It is observed that the omnidirectional behavior of radiation pattern is distorted at higher resonant frequencies compared to lower resonant frequencies. These changes are noticed because of change in the nature of current from standing wave at lower resonant frequencies to travelling wave at higher resonant frequencies. The measured gain of the proposed UMA at both ports is carried out as displayed in Figure 9(a). Here, in the gain measurement when port 1 is excited then port 2 is matched with 50 Ω load, and vice versa. It is observed from the gain response of the UMA antennas that gain variation is within a 3 dB range and shows a significant suppression in the WLAN notch band. The measured gain varies in the range of 1.8 to 4.7 dBi.

3.3. Diversity Performance

The envelope correlation coefficient (ECC) is an important constraint to analyze the diversity characteristics of a wideband MIMO antenna [21–23]. It is evaluated with the help of S-parameters as given in [13, 21]:

$$\rho_e = \frac{|S_{11}^* S_{12} + S_{21}^* S_{22}|^2}{(1 - (|S_{11}|^2 + |S_{21}|^2))(1 - (|S_{22}|^2 + |S_{12}|^2))} \tag{4}$$

The ECC of the proposed UMA is displayed in Figure 9(b). It can be seen that its value is always smaller than 0.01 within the entire UWB because of efficient design of the presented antenna. Moreover, in order to get good diversity performance its calculated value should be smaller than its threshold value of 0.5 [13]. Similarly, the quality of UWB MIMO/diversity system in a rich multipath environment is

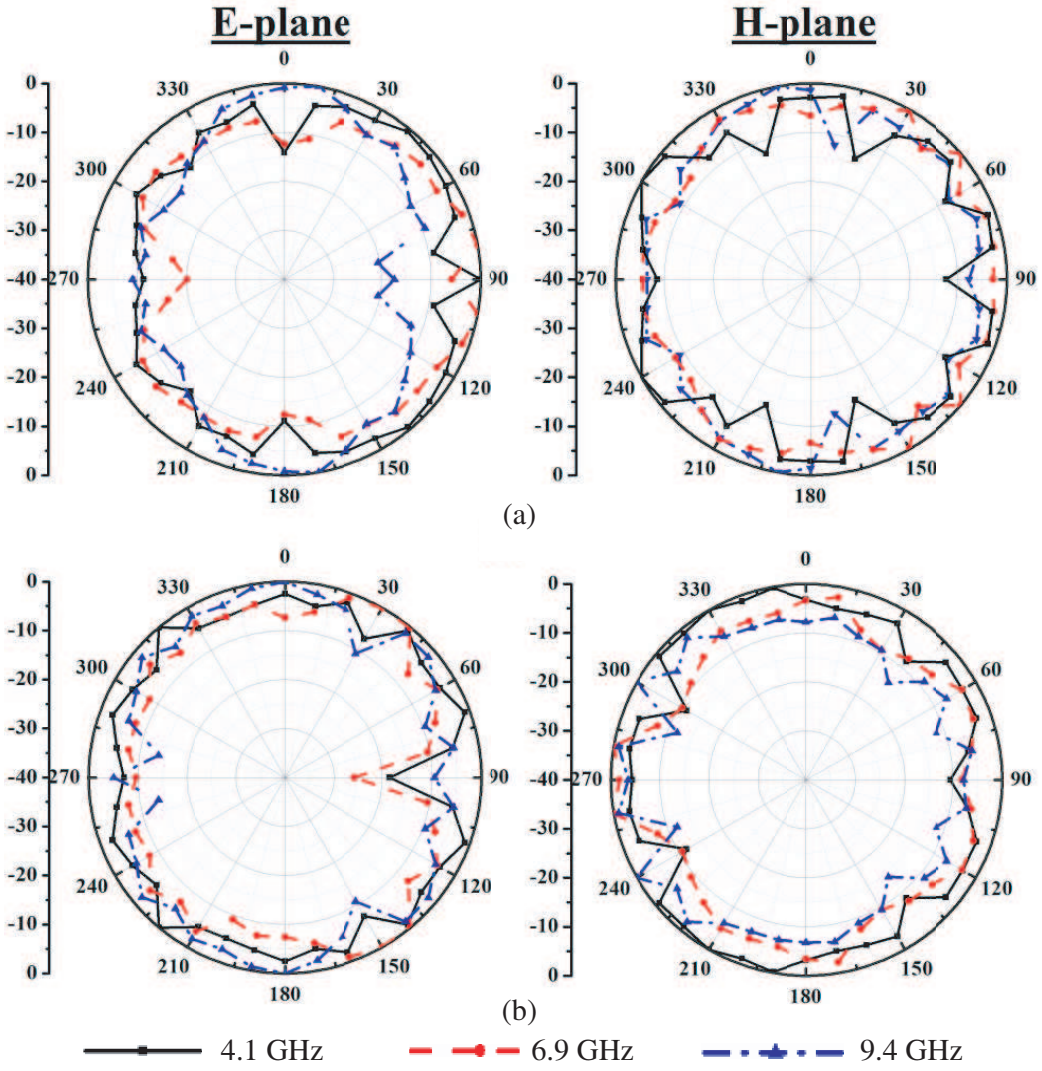

Figure 8. Radiation characteristics of the proposed antenna at 4.1 GHz, 6.9 GHz and 9.4 GHz in E-plane and H-plane (a) when port 1 is matched, (b) when port 2 is matched.

calculated in terms of another parameter, which is capacity loss (b/s/Hz). In a communication channel, capacity loss estimation helps to decide the upper bound of transmission rate, which in turn leads to reliable transmission. In case of a 2×2 MIMO/diversity antenna,capacity loss value should be less than the threshold 0.4 b/s/Hz [24, 25] and it is estimated mathematically by the correlation matrix as given in [25], using

$$C_{loss} = -\log_2 \det\left(\psi^R\right) \tag{5}$$

where, ψ^R shows the receiving antenna correlation matrix expressed as:

$$\psi^R = \begin{bmatrix} \rho_{11} & \rho_{12} \\ \rho_{21} & \rho_{22} \end{bmatrix}, \quad \rho_{ii} = 1 - \left(|S_{ii}|^2 + |S_{ij}|^2\right)$$

and $\rho_{ij} = -(S_{ii}^* S_{ij} + S_{ji}^* S_{ij})$, for $i, j = 1$ or 2.

The capacity loss behavior is also shown in Fig. 9(b). It can be seen that its value is less than 0.3 b/s/Hz (mostly less than 0.2 b/s/Hz), except in the WLAN notch band and that in the UWB spectrum, it is lower than the threshold value 0.4 b/s/Hz [25].

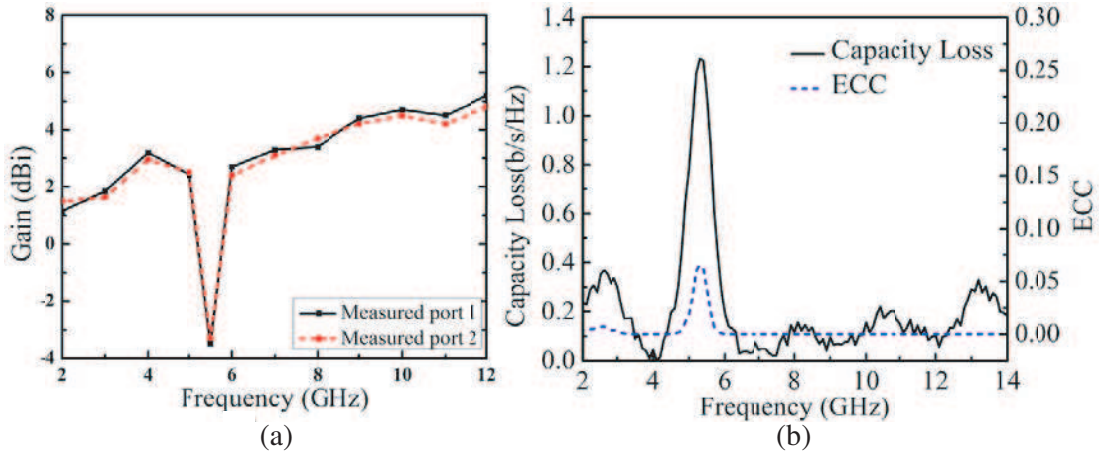

Figure 9. Results of the proposed UMA antenna, (a) gain and (b) ECC and capacity loss.

4. COMPARISON WITH OTHER UWB MIMO ANTENNAS

It is observed from Table 1 that the proposed antenna shows relatively better performance than other UMAs. The proposed UWB antenna structure provides a significant improvement in the performance, in terms of various parameters such as bandwidth, isolation, capacity loss, and diversity, compared to the other antennas in the literature [12].

Table 1. Comparison in terms of area occupied by UMA with other conventional and fractal antennas.

Antenna	This work	5	9	11	12	22	23	25
Size (mm^2)	29×38 $= 1102$	35×40 $= 1400$	48×48 $= 2304$	26×40 $= 1040$	26×38 $= 988$	23×29 $= 667$	23×39.5 $= 908.5$	100×50 $= 5000$
B.W. (GHz)	2.5–19	3.1–11.6	2.5–12	3.1–11	3.1–10.8	3–12	2.5–12	1.65-6.45
S_{21} (dB)	> 21.5	> 16	> 15	> 15	> 20	> 15	> 21	> 15
WLAN Band-notch	Yes	No	Yes	No	No	No	No	No
ECC	< 0.01	< 0.01	< 0.005	< 0.2	No	< 0.15	< -20 dB	< 0.04
Capacity Loss (b/s/Hz)	< 0.3	No	No	No	No	No	No	< 0.3

5. CONCLUSION

A compact UWB MIMO antenna with WLAN band-notch characteristics is presented, and its properties are studied. The introduction of a fractal slot in the ground plane of the antenna helps to improve the impedance bandwidth and enhance radiation characteristics. L-shaped, I-shaped grounded stubs and a rectangular slot are introduced in the design to achieve high isolation better than 21.5 dB and sharp band rejection, respectively. Moreover, performance of the presented structure in terms of other parameters, such as radiation pattern, antenna gain and ECC, is also studied and discussed. A comparative analysis of the antenna with other antenna structures is presented. Thus, the presented MIMO antenna is an appropriate candidate for portable UWB applications.

REFERENCES

1. FCC, Washington, DC, "FCC 1st report and order on ultrawideband technology," Feb. 2002.
2. Wallace, J. W. and M. A. Jensen, "Experimental characterization of the MIMO wireless channel," *IEEE Antennas and Propagation Society International Symposium*, Vol. 3, 92–95, Jul. 8–13, 2001.
3. Ben, I. M., L. Talbi, M. Nedil, and K. Hettak, "MIMO-UWB channel characterization within an underground mine gallery," *IEEE Trans. Antennas Propag.*, Vol. 60, No. 10, 4866–4874, 2012.
4. See, T. S. P. and Z. N. Chen, "An ultrawideband diversity antenna," *IEEE Trans. Antennas Propag.*, Vol. 57, No. 6, 1597–1605, 2009.
5. Zhang, S., Z. N. Ying, J. Xiong, and S. L. He, "Ultrawideband MIMO/diversity antennas with a tree-like structure to enhance wideband isolation," *IEEE Antennas Wireless Propag. Lett.*, Vol. 8, 1279–1232, 2009.
6. Li, L., Z. L. Zhou, J. S. Hong, and B. Z. Wang, "Compact dual-bandnotched UWB planar monopole antenna with modified SRR," *Electron. Lett.*, Vol. 47, No. 17, 950–951, 2011.
7. Kelly, J. R., P. S. Hall, and P. Gardner, "Band-notched UWB antenna incorporating a microstrip open-loop resonator," *IEEE Trans. Antennas Propag.*, Vol. 59, No. 8, 3045–3048, 2011.
8. Jiangand, W. and W. Q. Che, "A novel UWB antenna with dual notched bands for WiMAX and WLAN applications," *IEEE Antennas Wireless Propag. Lett.*, Vol. 11, 293–296, 2012.
9. Gao, P., S. He, X. Wei, Z. Xu, N. Wang, and Y. Zheng, "Compact printed UWB diversity slot antenna with 5.5-GHz band-notched characteristics," *IEEE Antennas Wireless Propag. Lett.*, Vol. 13, 376–379, 2014.
10. Lee, J.-M., K.-B. Kim, H.-K. Ryu, and J.-M. Woo, "A compact ultrawideband MIMO antenna with WLAN band-rejected operation for mobile devices," *IEEE Antennas Wireless Propag. Lett.*, Vol. 11, 990–993, 2012.
11. Li, L., S. W. Cheung, and T. I. Yuk, "Compact MIMO antenna for portable devices in UWB applications," *IEEE Trans. Antennas Propag.*, Vol. 61, No. 8, 4257–4264, Aug. 2013.
12. Wang, L., L. Xu, X. Chen, R. Yang, L. Han, and W. Zhang, "A compact ultrawideband diversity antenna with high isolation," *IEEE Antennas Wireless Propag. Lett.*, Vol. 13, 35–38, 2014.
13. Karaboikis, M. P., V. C. Papamichael, G. F. Tsachtsiris, C. F. Soras, and V. T. Makios, "Integrating compact printed antennas onto small diversity/MIMO terminals," *IEEE Trans. Antennas Propag.*, Vol. 56, No. 7, 2067–2078, Jul. 2008.
14. Zaker, R., C. Ghobadi, and J. Nourinia, "Novel modified UWB planar monopole antenna with variable frequency band-notch function," *IEEE Antennas Wireless Propag. Lett.*, Vol. 7, 112–114, 2008.
15. Amiri, S., N. Ojaroudi, F. Geran, and M. Ojaroudi, "A novel and compact monopole antenna with band-stop performance for UWB applications," *Telecommunications Forum (TELFOR)*, Vol. 20, 1156–1158, 2012.
16. Zaker, R., C. Ghobadi, and J. Nourinia, "Bandwidth enhancement of novel compact single and dual band-notched printed monopole antenna with a pair of L-shaped slots," *IEEE Trans. Antennas Propag.*, Vol. 57, 3978–3983, 2009.
17. Fereidoony, F., S. Chamaani, and S. A. Mirtaheri, "Systematic design of UWB monopole antennas with stable omnidirectional radiation pattern," *IEEE Antennas Wireless Propag. Lett.*, Vol. 11, 752–755, 2012.
18. Zhang, Y., W. Hong, C. Yu, Z. Q. Kuai, Y. D. Don, and J. Y. Zhou, "Planar ultrawideband antennas with multiple notched bands based on etched slots on the patch and/or split ring resonators on the feed line," *IEEE Trans. Antennas Propag.*, Vol. 56, No. 9, 3063–3068, Sep. 2008.
19. Pozar, D. M., *Microwave Engineering*, 2nd Edition, New York, 1998.
20. Bourke, P., "Circumference of an ellipse," 2013 [Online], Available: http://paulbourke.net/geometry/ellipsecirc/.
21. Tripathi, S., A. Mohan, and S. Yadav, "A compact octagonal fractal UWB MIMO antenna with WLAN band-rejection," *Microwave and Opt. Tech. Lett.*, Vol. 57, No. 8, 1919–1925, 2015.

22. Khan, M. S., A. D. Capobianco, S. M. Asif, D. E. Anagnostou, R. M. Shubair, and B. D. Braaten, "A compact CSRR enabled UWB MIMO antenna," *IEEE Antennas Wireless Propag. Lett.*, Vol. 58, No. 6, 808–812, 2016.
23. Khan, M. S., A. D. Capobianco, A. Naqvi, B. Ijaz, S. Asif, and B. D. Braaten, "Planar, compact ultra-wideband polarisation diversity antenna array," *IET Microwaves, Antennas and Propagation*, Vol. 9, No. 15, 1761–1768, Dec. 2015.
24. Li, J.-F., Q.-X. Chu, and T.-G. Huang, "A compact wideband MIMO antenna with two novel bent slits," *IEEE Trans. Antennas Propag.*, Vol. 60, No. 2, 482–489, 2012.
25. Choukiker, Y. K., S. K. Sharma, and S. K. Behera, "Hybrid fractal shape planar monopole antenna covering multiband wireless communications with MIMO implementation for handheld mobile devices," *IEEE Trans. Antennas Propag.*, Vol. 62, No. 3, 1483–1488, 2014.